Princeton Plasma Physics Laboratory

PPPL- 5065

Magnetic Diagnostics for Equilibrium Reconstructions with Eddy Currents on the Lithium Tokamak Experiment

J.C. Schmitt, J. Bialek,
S. Lazerson, and R. Majeski

SEPTEMBER 2014

Prepared for the U.S. Department of Energy under Contract DE-AC02-09CH11466.

Princeton Plasma Physics Laboratory
Report Disclaimers

Full Legal Disclaimer

Trademark Disclaimer

PPPL Report Availability

Princeton Plasma Physics Laboratory:

http://www.pppl.gov/techreports.cfm

Office of Scientific and Technical Information (OSTI):

http://www.osti.gov/scitech/

Related Links:

U.S. Department of Energy

Office of Scientific and Technical Information

Magnetic diagnostics for equilibrium reconstructions with eddy currents on the lithium tokamak experiment[a)]

J. C. Schmitt,[1,b)] J. Bialek,[2] S. Lazerson,[1] and R. Majeski[1]
[1]*Princeton Plasma Physics Laboratory, Princeton, New Jersey 08543, USA*
[2]*Department of Applied Physics and Applied Mathematics, Columbia University, New York, New York 10027, USA*

(Presented 5 June 2014; received 1 June 2014; accepted 23 July 2014; published online 11 August 2014)

The Lithium Tokamak eXperiment is a spherical tokamak with a close-fitting low-recycling wall composed of thin lithium layers evaporated onto a stainless steel-lined copper shell. Long-lived non-axisymmetric eddy currents are induced in the shell and vacuum vessel by transient plasma and coil currents and these eddy currents influence both the plasma and the magnetic diagnostic signals that are used as constraints for equilibrium reconstruction. A newly installed set of re-entrant magnetic diagnostics and internal saddle flux loops, compatible with high-temperatures and lithium environments, is discussed. Details of the axisymmetric (2D) and non-axisymmetric (3D) treatments of the eddy currents and the equilibrium reconstruction are presented. © *2014 AIP Publishing LLC*. [http://dx.doi.org/10.1063/1.4892159]

I. INTRODUCTION

The Lithium Tokamak eXperiment (LTX) is an Ohmically-heated spherical tokamak ($R_0 = 0.4$ m, $a = 0.26$ m, $\kappa \approx 1.6$, $B_0 = 0.17$ T) with a close-fitting low-recycling wall composed of thin lithium layers evaporated onto a stainless steel-lined copper shell. The copper shell is made of four quadrants with toroidal and poloidal breaks; each quadrant is 1 cm thick and has a 1.5 mm stainless steel liner explosively-bonded to the plasma-facing side. Figure 1 (top) shows a computer-aided design (CAD) drawing of the LTX device with a cutaway view to reveal the location of the shell. Figure 1 (bottom) shows a side view of the four quadrants and the toroidal and poloidal breaks. Each quadrant is fitted with resistive heaters to allow operations with the shell over a range of temperatures, from room temperature up to about 350 °C (Lithium melts at 180.5 °C). The entire surface area of the shell is approximate 5 m^3, or about 85% of the total surface area of the plasma.

The copper quadrants are good electrical conductors and the stainless steel vacuum vessel (VV) is electrically continuous in the toroidal and poloidal directions. In the presence of time-changing coil and plasma currents that are typical throughout the plasma discharge, eddy currents are induced in the shell and VV. Neither the shell nor the VV are axisymmetric so the eddy currents induced within these structures are intrinsically 3D in nature. These long-lived eddy currents affect tokamak startup, operations, and equilibrium reconstructions. In this paper, the diagnostics and modeling strategies to study these eddy currents and their effect on the plasma equilibrium are discussed.

This paper is organized as follows. The magnetic diagnostics are described in Sec. II. Section III discusses the eddy currents in the conducting structures around the plasma and their treatment by two different methods: a 2D axisymmetric model and a 3D thin-shelled model. The next steps for the reconstruction process are discussed in Sec. IV.

II. MAGNETIC DIAGNOSTICS

Diagnostic access to the plasma is limited to the toroidal and poloidal breaks in the copper shell. Furthermore, the copper shell is heated at times to maintain the evaporated lithium in a liquid state and internal diagnostics will be exposed to lithium. Hundreds of thermal cycles, extended lithium exposure and unforeseen JxB forces which cause the copper shell to move during each shot have impacted the design of internal diagnostics. The original set of internal magnetic sensors on LTX[1] can be divided into two groups: those that measure the magnetic field (1) over large toroidally- or poloidally-averaged regions, such as poloidal or toroidal flux loops, or (2) locally, either point-like or non-toroidally averaged measurement such as local B sensors or saddle flux loops with finite toroidal and poloidal extant. In LTX, the first group has survived the thermal cycling and lithium exposure because the sensor wires were completely shielded by stainless steel tubing from lithium exposure and their mounting hardware was not destroyed by the shell motion. The second group of diagnostics was almost completely rendered unusable. Lithium deposits on the sensor windings shorted out the local B sensors and the shell motion destroyed the mounting hardware of the saddle flux loops.

New magnetic diagnostics were installed during the maintenance period to replace those that were destroyed. New local B sensors (Ref. 2, Chap. 2) were installed in reentrant thin-walled (0.020 in.) stainless steel tubes to protect them from lithium exposure. The skin time of the tubes is about 1.4 μs, which is a negligible effect for reconstructions that will use signals averaged over the timescale of a millisecond. The maximum temperature of the interior of the tubes was

[a)]Contributed paper, published as part of the Proceedings of the 20th Topical Conference on High-Temperature Plasma Diagnostics, Atlanta, Georgia, USA, June 2014.

[b)]Author to whom correspondence should be addressed. Electronic mail: jschmitt@pppl.gov

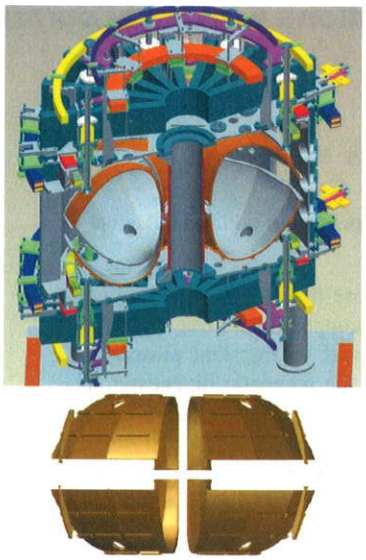

FIG. 1. (Top) Cutaway view of LTX revealing the vacuum vessel, field coils, and the stainless steel lined copper shell. (Bottom) Side view of the four shell quadrants and the poloidal and toroidal breaks.

measured to be about 150 °C when the shells were heated to 350 °C. The sensors are compatible with these temperatures: They are constructed of polyimide-coated 38 AWG wire (rated to 240 °C) wound on high-temperature glass-filled PEEK (rated to 250 °C) and potted in 300 °C-rated epoxy. Each sensor has an effective turns-area product, NA $\approx$ 19.6 $\times$ 10^{-3} m^2. Three sensors are installed into a single PEEK form (a "triplet") to measure changes in the local magnetic field in three orthogonal directions, Figure 2. A total of 18 triplets are installed around the plasma (poloidally) at a single toroidal location in the center of one of the toroidal breaks in the copper shell. A line drawing of the position and normal direction of each sensor is shown in Figure 3. The signals from each sensor are integrated electronically with channel dependent gain factors ranging from 600 to 1500 s^{-1} and recorded by 16-bit D-tAcq digitizers at a sampling rate of 100 kHz. The minimum measurable field is typically between 0.1 and 0.2 G.

Six saddle flux loops were also installed. These loops are particularly useful in measuring the fields due to eddy currents in the copper shell. Each saddle loop is made of two turns of a copper wire which is insulated by a layer of fiberglass and a stainless steel braid. The turns are attached to a stainless steel form which attaches on one side to a single shell quadrant, so that they are not subject to forces that would otherwise twist and damage their supporting connection. The wire leads

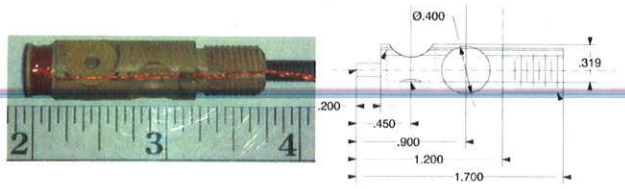

FIG. 2. (Left) Reentrant B sensors mounted in PEEK form. (Right) CAD sketch of PEEK form. Dimensions in inches.

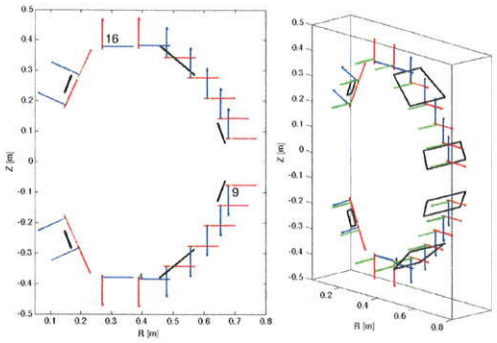

FIG. 3. Line drawing of the locations of the newly installed reentrant B sensors and saddle flux loops installed at one of the toroidal breaks. The normal direction of the B sensors is indicated by the red, blue, and green arrows. The outline of the saddle flux loops is shown in black.

are connected to a vacuum electrical feedthrough and the signals are integrated electronically with gain factors of 500–10 000 s^{-1}. The locations of these loops are shown in black in Figure 3. There are three located in the top half and three in the bottom half. Two are located on the inboard side of the plasma, two are located near the outboard side of the plasma, and two are placed near the top/bottom of the plasma, in between the inboard and outboard loops. The areas of the inboard, middle, and outboard loops are 16 cm^2, 211 cm^2, and 128 cm^2, respectively.

An effective calibration factor, which accounts for variations in NA and integrator gains, for each of the new B sensors and saddle loops was determined through a series of long-pulse vacuum magnetic field tests. Various combinations of field coils on LTX were energized with 100's to 1000's of Amperes of current for long times, typically 400 ms, to allow induced eddy currents in the copper shell and VV to decay to minimal levels. The measured response late in the shot was compared to an ideal response calculated by a Biot-Savart code. For each diagnostic, the calibration factor for many different coil combinations was calculated: the mean value is used as the calibration factor and standard deviation (typically 5%) provides a sense of it relative precision.

The rest of the magnetic diagnostics on LTX are discussed Ref. 1. The total set of magnetic diagnostics for equilibrium reconstructions includes 26 poloidal flux loops (8 on the upper shells, 8 on the lower shells, 10 along the centerstack), 1 toroidal (diamagnetic) flux loop, 6 saddle coils, 18 B-dot triplets (3-axis), and 26 single-axis B-dot coils located close to the vacuum vessel.

III. EDDY CURRENTS

Transient coil and plasma currents induce eddy currents in the non-axisymmetric copper shell and VV. Two approaches for including these eddy currents in the equilibrium reconstruction process are discussed below. The first approach is with a 2D axisymmetric model of the plasma and surrounding conducting structure. The second approach couples a 3D calculation of the eddy current distribution with a 3D equilibrium reconstruction code to explore possible non-axisymmetric effects of the eddy currents.

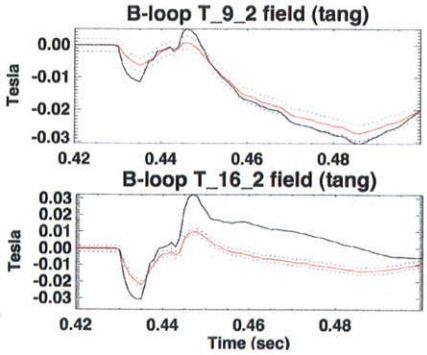

FIG. 4. The measured (red) and LRDFIT-calculated (black) signals for a vacuum, (coils-only) shot in LTX. The top (bottom) plot corresponds to sensor #9 (#16) in Figure 3, with the normal direction indicated by the blue arrow in that figure.

A. LRDFIT

LRDFIT (LR circuit model with Data FITting capabilities) was previously adapted for use on LTX.[3] In LRDFIT, field coils, plasma and nearby conducting structures (shells and VV) are modeled as axisymmetric conducting regions and the toroidal currents in these regions are determined self-consistently with an inductive-resistive (L-R) circuit model. It is capable of reconstructing toroidal currents constrained by measured signals. One method uses a singular-value decomposition (SVD), which neglects details of force-balance in the plasma. The second method includes the physics of the Grad-Shafranov equation (GSE) in the reconstruction.

Physically, the shells and VV of LTX are not axisymmetric. The shell has poloidal and toroidal breaks, the VV has large non-axisymmetric ports, and the eddy currents are intrinsically 3D. However, LRDFIT assumes axisymmetric structures and does not capture the poloidal return currents along the edges of the quadrant or any toroidal variations in the eddy current distribution. To achieve better agreement between the measured and modeled magnetic sensors for vacuum (field coils only) shots, additional modifications were made to the LTX model. The conductivity of the shell was modified such that the inboard (outboard) sections had lower

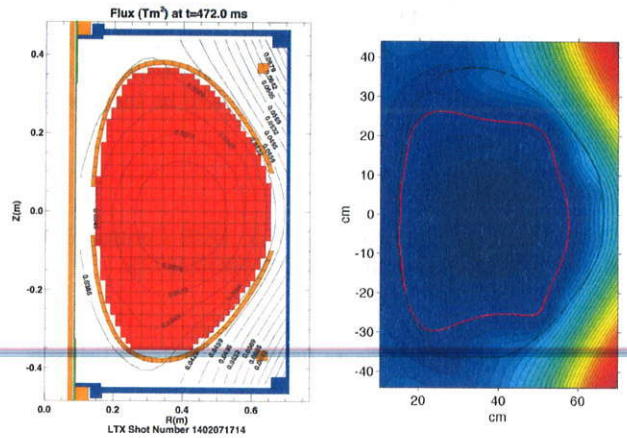

FIG. 5. Poloidal flux contours calculated by LRDFIT with SVD (left) and GSE (right) fits. The LCFS calculated by the GSE fit is outlined in red.

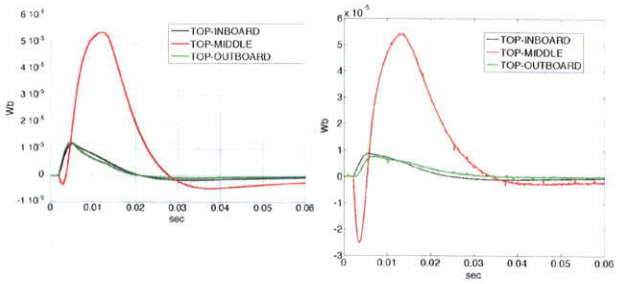

FIG. 6. Simulated saddle flux loops signals from VALEN (left) and the measured response (right) for a PF-only vacuum shot.

(higher) electrical conductivity, and a condition of zero net toroidal current in the shell was enforced. This improved the agreement for some sensors on longer timescales (>50 ms), but differences between the measured and modeled signals were still present for shorter timescales (<50 ms). Examples are shown in Figure 4 for a typical coils-only vacuum shot. Sensor #9 (T_9_2), whose position is shown in Figure 3 with its normal direction in blue, is modeled reasonably well by LRDFIT. Sensor #16 (T_16_2), also shown in Figure 3 with its normal direction in blue, is modeled very poorly. Plasmas are typically formed from 445 ms to about 480 ms, so the level of disagreement shown makes sensors like this problematic for LRDFIT reconstruction constraints.

Regardless, because of its rapid execution, LRDFIT can still be a useful tool for LTX operations. Both SVD and GSE fits are functional for LTX, provided that only certain subsets of magnetic diagnostics are used as fitting constraints. Contours of poloidal flux from SVD and GSE fits for a typical LTX plasma are shown in Figure 5. The induced eddy currents in the shells for this particular shot are in the 10's of kA range, and decay over time during the shot, but do not reach zero (not shown).

B. VALEN

The VALEN code[4] is used to calculate the 3D eddy current in the shell and VV of LTX. The conducting structures are modeled as thin shells using a L-R circuit formulation. Eigenvalue and eigenvector information is available from this code. Initial calculations with VALEN indicated that the

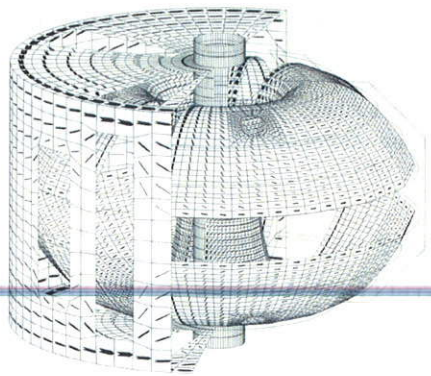

FIG. 7. Eddy current distribution at 2.5 ms after the PF coils are energized for coils-only shot.

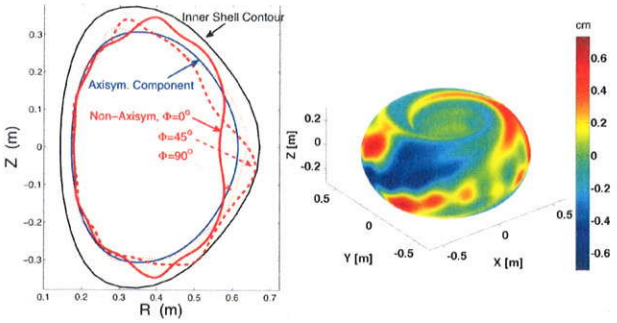

FIG. 8. (Left) The VMEC fixed-boundary LCFS and inner shell contour are shown in black. For a VMEC free-boundary calculation, the axisymmetric (N = 0) component of the LCFS is shown in blue. The non-axisymmetric LCFS is shown at Φ = 0°, 45°, and 90° in red as solid, dashed, and dotted lines, respectively. The N ≠ 0 components are exaggerated by ×10. (Right) The displacement of the LCFS (in cm) from the N = 0 component is mapped onto the N = 0 surface. Φ = 0° is along the +X-axis through Y = 0.

slowest eigenvector of the shell couples with the poloidal field (PF) coils with a characteristic eigenvalue of about 50 ms, which is comparable to the PF coil ramp rate and plasma duration. Time domain simulations are used to calculate the eddy current response due to transient currents in the poloidal and toroidal field coils as well as the plasma. The magnitude and spatial distribution of the non-axisymmetric eddy current vary with time and are located very close to the plasma so a 3D equilibrium reconstruction is required to capture these details.

A series of vacuum (coils-only) shots were used to validate the use of VALEN for LTX. One example shown here is where a pair of PF coils were energized and the measured coil currents were used as inputs into VALEN. The calculated response (VALEN output) for the upper saddle flux loops is shown in Figure 6 (left) and the measured response is shown in Figure 6 (right). The level of agreement between the simulation and measurement is excellent. There are some minor differences between the signals for the first few ms, which is likely due to finite-thickness effects that are not captured in the thin-shell assumption in VALEN. The calculated distribution of the eddy currents in the shells and VV 2.5 ms after the start of the coil excitation is shown in Figure 7.

For plasma discharges, the measured coil currents and the measured net toroidal plasma current are both included in the eddy current calculation. The plasma current is simplified by modeling it as a uniform current density over a circular cross-sectional axisymmetric torus with minor radius 24 cm and major radius 40 cm, which is the approximate location of the bulk plasma current based on preliminary LRDFIT reconstructions.

C. STELLOPT

The STELLOPT[5] code uses VMEC[6] to calculate the MHD equilibrium in a 3D toroidal geometry using Fourier expansions in the poloidal and toroidal direction for flux-surface quantities. STELLOPT can use magnetic sensor signals as constraints for equilibrium reconstruction. Typically, the magnetic field due to field coils, prescribed in a "mgrid" file, is used as the background field for VMEC calculations. Here, the magnetic field due to eddy currents calculated by VALEN is included in the mgrid file so that the eddy field is included in the MHD equilibrium calculation. The total (net) magnetic field in LTX, including the contribution from the eddy currents is approximately stellarator-symmetric with small error fields.[7] Initial calculations of LTX fixed- and free-boundary plasma equilibria have been completed. The axisymmetric fixed-boundary solution (which neglects eddy currents) is defined to have its last-closed flux surface (LCFS) be the same as the inner contour of the copper shell and is shown in Figure 8 (left) in black. A free-boundary solution, which includes the vacuum magnetic field and the effects of the calculated eddy currents due to both the field coils and an axisymmetric plasma current is also shown. The axisymmetric N = 0 component of the LCFS is shown in blue. The non-axisymmetric LCFS at Φ = 0°, 45°, and 90° is shown in red solid, dashed, and dotted lines, respectively. The N ≠ 0 components have been exaggerated by a factor of 10. The displacement of the LCFS from the N = 0 component is mapped onto the N = 0 surface in Figure 8 (right) and has an N = 2 characteristic. The displacement varies from −0.7 cm to 0.7 cm.

It should be noted that this is not a self-consistent calculation of the plasma equilibrium with the eddy currents in the sense that the modifications to the plasma column current are not included in the eddy current calculation. The eddy currents in the shell and VV were calculated based on the measured coil currents and with the assumption of a uniform plasma current density located within a region inside of the confinement volume. Including the effects of non-axisymmetric plasma current distributions on the eddy currents is beyond the scope of this work.

IV. FUTURE STEPS

The next step is to begin equilibrium reconstructions with STELLOPT. The impact of fields due to 3D eddy currents will be evaluated by comparing the results of the axisymmetric (2D) LRDFIT and (3D) STELLOPT reconstructions. The present set of magnetic diagnostics is located at only a single toroidal plane, so at this point, only comparisons of the N = 0 nature of the plasma column can be studied. In the future, additional magnetic diagnostics at other toroidal locations will be installed, and internal plasma measurements (Thomson, ChERS, interferometry, etc.) will be included as reconstruction constraints.

ACKNOWLEDGMENTS

This work was supported by U.S. DOE Contract Nos. DE-AC02-09CH11466 and DE-AC05-00OR22725.

[1]L. Berzak *et al.*, Rev. Sci. Instrum. **81**, 10E114 (2010).
[2]I. Hutchinson, *Principles of Plasma Diagnostics* (Cambridge University Press, 2002).
[3]L. Berzak Hopkins *et al.*, Nucl. Fusion **52**, 063025 (2012).
[4]J. Bialek *et al.*, Phys. Plasmas **8**, 2170 (2001).
[5]D. A. Spong *et al.*, Nucl. Fusion **41**, 711 (2001).
[6]S. P. Hirshman and J. C. Whitson, Phys. Fluids **26**, 3553 (1983).
[7]R. L. Dewar and S. R. Hudson, Physica D **112**, 275 (1998).

Princeton Plasma Physics Laboratory
Office of Reports and Publications

Managed by
Princeton University

under contract with the
U.S. Department of Energy
(DE-AC02-09CH11466)

P.O. Box 451, Princeton, NJ 08543
Phone: 609-243-2245
Fax: 609-243-2751

E-mail: publications@pppl.gov
Website: http://www.pppl.gov